



# HHS Public Access

Author manuscript

*Curr Biol.* Author manuscript; available in PMC 2020 May 20.

Published in final edited form as:

*Curr Biol.* 2019 May 20; 29(10): 1660–1668.e4. doi:10.1016/j.cub.2019.03.004.

## Diverse food-sensing neurons trigger idiothetic local search in *Drosophila*

Román A. Corfas, Tarun Sharma, and Michael H. Dickinson<sup>1,\*</sup>

Division of Biology & Bioengineering, California Institute of Technology, 1200 East California Blvd., Pasadena CA 91125, USA

### SUMMARY

Foraging animals may benefit from remembering the location of a newly discovered food patch while continuing to explore nearby [1, 2]. For example, after encountering a drop of yeast or sugar, hungry flies often perform a local search [3, 4]. That is, rather than remaining on the food or simply walking away, flies execute a series of exploratory excursions during which they repeatedly depart and return to the resource. Fruit flies, *Drosophila melanogaster*, can perform this food-centered search behavior in the absence of external landmarks, instead relying on internal (idiothetic) cues [5]. This path integration behavior may represent a deeply conserved navigational capacity in insects [6, 7], but its underlying neural basis remains unknown. Here, we used optogenetic activation to screen candidate cell classes and found that local searches can be initiated by diverse sensory neurons. Optogenetically induced searches resemble those triggered by actual food, are modulated by starvation state, and exhibit key features of path integration. Flies perform tightly centered searches around the fictive food site, even within a constrained maze, and can return to the fictive food site after long excursions. Together, these results suggest that flies enact local searches in response to a wide variety of food-associated cues, and that these sensory pathways may converge upon a common neural system for navigation. Using a virtual reality system, we demonstrate that local searches can be optogenetically induced in tethered flies walking on a spherical treadmill, laying the groundwork for future studies to image the brain during path integration.

### eTOC Blurb

After finding a patch of food, flies use path integration to execute a local search. Using optogenetic activation, Corfas et al. show that a variety of food-associated neurons trigger this

\*Correspondence: flyman@caltech.edu.

<sup>1</sup>Lead Contact

#### AUTHOR CONTRIBUTIONS

RAC conducted all experiments, except those in Figure 4 which were performed by TS. RAC analyzed all data and prepared all figures. RAC and MHD conceived of experiments and wrote the paper.

**Publisher's Disclaimer:** This is a PDF file of an unedited manuscript that has been accepted for publication. As a service to our customers we are providing this early version of the manuscript. The manuscript will undergo copyediting, typesetting, and review of the resulting proof before it is published in its final citable form. Please note that during the production process errors may be discovered which could affect the content, and all legal disclaimers that apply to the journal pertain.

#### DECLARATION OF INTERESTS

The authors declare no competing interests.

behavior, and that flies can perform searches within a maze or a virtual environment. The results pave the way for studying the neural basis of path integration.

## RESULTS & DISCUSSION

### An optogenetic screen identifies sugar-sensing neurons that elicit local search

To discover sensory pathways triggering local search, we tracked the behavior of individual female flies as they explored a circular arena with a featureless optogenetic activation zone at its center (Figure 1A). The assay consists of an initial 10-minute baseline control period, followed by a 30-minute period during which animals receive a 1-second pulse of red light (628 nm) whenever they enter the activation zone. For flies expressing the light-sensitive channel CsChrimson in food-sensing neurons, the activation zone should act as a patch of fictive food, potentially able to elicit a local search. Using this setup, we screened gustatory, olfactory, and reward-signaling neurons to identify cell classes that trigger local search. Aside from the light pulses used for optogenetic activation, the animals are in complete darkness and must rely on internal cues to navigate the open-field portion of the arena. To examine whether flies were conducting local search, we analyzed trajectories beginning at the activation zone and ending at the arena edge. Prior to testing, flies were subjected to 33–42 hours of starvation, during which they had access to water only.

It is known that flies perform local searches after discovering a drop of sucrose [3–5, 8–10], suggesting that sweet-sensing neurons may be sufficient to initiate this behavior. To test this, we used *Gr43a-GAL4>UAS-CsChrimson* flies to activate fructose-sensing neurons whenever the flies entered the activation zone [11, 12]. Activation of these gustatory neurons triggered local searches remarkably similar to those previously observed in response to actual food, consisting of a series of excursions from and returns to the fictive food site (Figures 1B, 1C and S1A–S1C; Video S1) [5]. Unlike parental controls, *Gr43a-GAL4>UAS-CsChrimson* flies extensively searched the area surrounding the activation zone (~30 cm<sup>2</sup>), after receiving a light-pulse (Figures 1D and 1E). These search trajectories were highly centered at the activation zone (Figures 1F and 1H) and consisted of numerous revisits to the activation zone (Figures 1G, 1I) — both features of local searches shown to require path integration [5]. During local search, flies cumulatively walked ~30–300 cm (approximately 100–1000 body lengths) before eventually straying to the arena edge (Figure 1J). Prior studies, using another *Gr43a-GAL4* line, suggest that *Gr43a* is expressed in neurons of the pharynx and brain that measure post-ingestive sugar levels, in addition to sugar-sensing neurons in the periphery [12]. However, we found that nearly identical local searches are triggered by activation using the *Gr5a-GAL4* driver, which only labels peripheral sugar-sensing neurons (Figures 1D–1J, S2A–S2D; Video S1) [13, 14]. Therefore, non-pharyngeal sugar sensors are capable of eliciting local search. This result is in disagreement with recent experiments suggesting that only pharyngeal sugar sensors can trigger local search [10]; however, that study did not examine the effect of activating specific subsets of sugar-sensing neurons. The use of fictive food in our experiments provides further evidence that flies are in fact using idiothetic path integration during local search, rather than relying on external (allothetic) cues coming from an actual drop of food such as visual

appearance, odor or humidity gradients, or tracks of food residue deposited during prior search excursions.

Previous work has shown that, compared to sucrose-triggered searches, a drop of 5% yeast solution elicits search trajectories that are even longer and include more revisits to the food [5, 15], suggesting that proteinaceous food components may also initiate this behavior. Amino acids present in yeast are a coveted source of nutrition for mated females, which require a protein source to produce eggs [16–18]. The ionotropic receptor *Ir76b* has been implicated in the detection of the taste of yeast [19], amino acids [20, 21], carbonation [22], and other important nutrients such as salt [23], polyamines [24], and fatty acids [25]. We tested *Ir76b-GAL4>UAS-CsChrimson* flies in our assay, and found that activation of these amino-acid sensors resulted in a modest increase in residence near the activation zone (Figures 1D and 1E), due largely to the animals ceasing locomotor activity (see results below). However, the activation did not trigger a local search — the trajectories covered little distance and rarely included a revisit to the activation site (Figures 1I, 1J and S2A–S2D). The failure to elicit local searches via activation of *Ir76b-GAL4* may be due to the fact that this line labels a large population of neurons associated with diverse sensory functions [19, 22]. Indeed, whereas silencing of these neurons disrupts preference for feeding on yeast, direct activation of *Ir76b-GAL4* neurons has never been shown to trigger feeding behavior [19].

Food odorants also trigger search behavior in insects. In flight, for example, encounters with an odor plume elicit the stereotyped cast and surge maneuvers that enable insects to localize the source of an advected odor [26, 27]. Recent studies have demonstrated that this also occurs during walking — flies increase their turn rate when they exit a plume of apple cider vinegar (ACV) odor [28, 29]. Attraction to the smell of ACV in *Drosophila* is mediated primarily by neurons expressing the olfactory receptor *Or42b* [30]. Optogenetic activation of *Or42b-GAL4* neurons produces attraction behavior in flies [31], as does activation of *Or59b-GAL4* neurons [32], which respond to acetate esters found in food odors [33, 34]. Simultaneous optogenetic activation of nearly all the olfactory receptor neurons via *Orco-GAL4* also produces attraction in flies [31]. We tested whether these three classes of olfactory neurons could trigger a local search and found that activation of *Orco-* and *Or59b-GAL4* neurons did not elicit searches (Figures 1D–1J and S2A–S2D). Activation of ACV-odor-sensing *Or42b-GAL4* neurons resulted in increased residence near the activation zone (Figures 1D, 1E and S2A–S2D) much like *Ir76b-GAL4*, but did not produce local searches according to our metrics (Figures 1H and 1J).

Next, we tested whether the water content of food drops might be enough to evoke local search. In *Drosophila*, water sensation is mediated by the osmosensitive ion channel *ppk28*, a member of the degenerin/epithelial sodium channel family [35]. We found that activation of water-sensing *ppk28-GAL4* neurons in food-deprived flies did not result in local search (Figures 1D–1J and S2A–S2D). This result is in agreement with previous behavioral experiments showing that *Drosophila* do not produce local search bouts after encountering a drop of pure water [5, 9].

We hypothesized that reward-signaling neurons of the central nervous system might also trigger local searches. Neuropeptide-F (NPF) is a highly conserved hunger-signaling neuropeptide that stimulates a variety of *Drosophila* behaviors, including feeding [36]. *NPF-GAL4* labels neurons in the posterior region of the *Drosophila* brain, and activation of these cells is rewarding in the context of olfactory conditioning [37]. We found that, much like *Ir76b-GAL4* and *Or42b-GAL4*, activation of *NPF-GAL4* neurons results in a modest increase in residence near the activation zone (Figures 1D, 1E and S2A–S2D), but not statistically significant local searches (Figures 1H and 1J). Another set of reward-signaling neurons are the dopaminergic protocerebral anterior medial (PAM) neurons, which are activated by sugar ingestion and innervate the mushroom body, a structure critical for forming associative memories [38, 39]. Activation of PAM neurons via *R58E02-GAL4* is known to mediate reward during olfactory conditioning [38, 39], and silencing PAM neurons inhibits food occupancy during foraging [40]. However, we found that activation of *R58E02-GAL4* neurons does not produce search behavior (Figures 1D–1J and S2A–S2D).

### Diverse food-sensing neurons trigger local searches modulated by starvation state

Because local searches are initiated by activation of sugar-receptors, we hypothesized that starvation state may influence the extent of optogenetically induced searches. The influence of starvation has been observed for sucrose-induced searches in *Drosophila* [9] as well as protein- and water-induced searches in the blowfly (*Phormia regina*) [15]. Until this point, all of our experiments were conducted with animals allowed access only to water for 33–42 hours preceding the trial. To examine the importance of starvation in promoting local search, we tested activation of sugar-sensing *Gr43a-GAL4* neurons in flies that were reared continuously on food or starved for only 9–18 hours. As expected, we found that longer starvation times result in more extensive searches, with longer trajectories and more revisits to the activation zone (Figures 2A–2D).

We next tested whether additional food deprivation could produce searches triggered by sensory pathways that had weak behavioral effects in our original screen. For these experiments, we starved flies for 7 days: 5 days with access to sucrose solution followed by 2 days with access to only water. Even in 7-day-starved animals, activation of amino acid-sensing *Ir76b-GAL4* neurons did not elicit substantial local search (Figures 2E–2G and S3A–S3D), despite the fact that protein-deprived mated females are known to develop a strong preference for amino acid-containing food [16–18]. However, we found that activation of ACV-odor-sensing *Or42b-GAL4* neurons in 7-day-starved animals resulted in extensive and centralized local searches, comparable to those triggered by sugar-sensing neurons (Figures 2E–2F, 2H, and S3A–S3D; Video S2). This finding is consistent with work showing that starvation promotes food search behavior in *Drosophila*, and that this effect is mediated by neuropeptidergic modulation of *Or42b-GAL4* neuron activity [41]. We also observed local search triggered by activation of *NPF-GAL4* neurons in 7-day-starved animals (Figures 2E–2F, 2I, and S3A–S3D; Video S2). This effect may be related to previous work showing that *NPF-GAL4* neurons are activated by food odors in a starvation-dependent manner [42]. Finally, we found that nutritional deprivation can even produce searches triggered by water-sensation — activation of *ppk28-GAL4* neurons elicited robust

local searches in animals subjected to a desiccating environment without food or water, (Figures 2E–2F, 2J, and S3A–S3D; Video S2).

Collectively, these results show that optogenetic activation of a variety of food-associated sensors can trigger searches, and that this behavior is influenced by the internal nutritional state, much like searches triggered by actual food. Previous work has shown that flies regulate their consumption of sugar and yeast depending on whether they are deficient in that specific nutrient [19]. When a fly finds a patch of yeast, for example, its decision to stay or leave depends strongly on whether it is deficient in amino acids [43]. Thus, it may be that flies only perform local search when they experience a food cue associated with a nutrient they currently need. To test this hypothesis further, we starved animals on a synthetic food medium [44] that allowed us to deprive flies specifically of either sugar or protein, while supplying them with an otherwise complete and balanced diet. Activation of *Gr43a-GAL4* sugar-sensors produced robust local searches in animals subjected to sugar-deprivation, but not in animals subjected to long-term protein-deprivation (Figures S3E–S3F, S3I–S3J), suggesting that sugar-sensation-triggered searches are a response to a specific nutritional need. However, activation of ACV-odor-sensing *Or42b-GAL4* neurons did not elicit searches in protein-deprived flies, and elicited modest searches in sugar-deprived flies (Figures S3G–S3J). However, as discussed above, activation of *Or42b-GAL4* neurons does elicit robust searches in 7-day-starved animals subjected to a combination of sugar and protein deprivation (Figures 2E–2F, 2H, and S3A–S3D; Video S2). One possible functional explanation for these differing results is that substances sensed via contact, such as sugar or water, produce local search conditional on the specific internal state of that nutrient. In contrast, because the detection of volatile compounds is a less reliable indicator of the nutritional content of nearby food, the potency with which an odor can elicit local search may depend on the general nutritional state of the animal. Determining the ethological connection between food-triggered search and nutrient homeostasis will require further investigation.

In his initial description of food-induced local search, Dethier demonstrated that when a hungry blowfly discovers a drop of food, it performs a proboscis extension response (PER) — a reflex associated with appetitive cues [3, 4]. To explore the role of proboscis extension in optogenetically induced local search, we tested whether activation of each of these neuron classes elicits PER. As has been previously reported, activation of sugar-sensing *Gr5a-GAL4* neurons elicits PER (Figure S4A) [45–47]. We found that activation of *Gr43a-GAL4* neurons also elicits PER in a starvation-dependent manner (Figure S4A), indicating that fructose triggers a feeding reflex similar to that of other sugars. Activation of water sensors via *ppk28-GAL4* neurons also resulted in PER, even in animals that had not been subjected to dry-starvation (Figure S4A). We also found that activation of hunger-signaling neurons via *NPF-GAL4* elicited strong PER (Figure S4A), demonstrating a novel function for these neurons. However, none of the other neuron classes in our screen consistently triggered PER, including *Or42b-GAL4* neurons (Figure S4A), indicating that local search can be initiated by receptors that do not by themselves elicit PER.

Together, these results suggest that local searches are triggered by both contact chemosensory cues that signal that the fly is on food (e.g. water or sugar), as well as volatile

cues that indicate food is nearby (e.g. the odor of ACV). It appears that flies even initiate local searches around a location associated with a rewarding stimulus (i.e. activation of *NPF-GAL4* neurons) without accompanying activation of peripheral chemosensors. Although searches triggered by sugar, water, odor, and reward-signaling appear broadly similar in our experiments (Figures 1C, 2H and 2J), it is likely that their underlying behavioral structure differs [28, 48]. For example, we found that whereas activation of *Gr43a*-, *Gr5a*-, *Ir76b*-, *ppk28*-, or *NPF-GAL4* results in decreased locomotion or complete stopping, activation of ACV-odor-sensing *Or42b-GAL4* neurons only elicits a brief startle response, similar to controls (Figures S4B and S4C). The absence of slowing at the initiation of searches triggered by *Or42b-GAL4* neurons is consistent with the interpretation that these searches are related to the casting behaviors elicited by loss of an odor plume [26, 27, 29]. Future studies using our paradigm may determine whether local searches triggered by distinct food-associated stimuli are stereotyped, or are instead accomplished through diverse behavioral strategies.

### Optogenetically induced local searches provide a model system for the study of insect path integration

Our results show that optogenetically induced local searches resemble those evoked by actual food, suggesting that flies are using idiothetic path integration to keep track of their position relative to the activation zone. Unlike previous studies using real food [3–5, 8–10], we are able to monitor every occasion that the fly senses the fictive food and can easily reinforce the memory of its location. Using the data from *Gr43a-GAL4>UAS-CsChrimson* animals in our original screen (Figure 1), we examined the search trajectories occurring after each optogenetic stimulation. Many of these trajectories lasted only a few seconds and covered only a few centimeters before the fly returned to the activation zone thus receiving another optogenetic pulse (Figures 3A and 3B). In many cases, however, flies performed a centered local search lasting minutes and covering hundreds of body lengths without an intervening optogenetic stimulation (Figures 3A–3C). This implies that a persistent internal representation of space underlies this behavior — without sustaining a centered search, flies would quickly stray to the arena edge. We also observed that flies can update the center of their search upon discovering another activation zone (Figures 3D–3F), as has been found with searches around real food [5]. Moreover, flies repeatedly shift the center of their search between activation zones (Figures 3D–3F), resembling experiments in which flies foraged among an array of food patches [43]. In those experiments, flies were found to execute local searches around food sites, but also discovered new food sites by exploring further — a behavior dependent on the internal nutrient state of the fly [43].

To explore the versatility of local search behavior, we investigated whether flies can execute path integration in a constrained environment, as opposed to an open field. Reminiscent of experiments done with foraging ants [49], we constructed a grid-shaped maze called Flyadelphia — a reference to Philadelphia’s canonical street grid — with an optogenetic activation zone at its center (Figure 3G). Remarkably, *Gr43a-GAL4>UAS-CsChrimson* animals were able to perform lengthy and elaborate local searches within this confined arena (Figure 3H; Video S3). In the absence of a light-pulse, flies typically walk through the activation zone and continue on a straight path until reaching the arena edge (Figures 3I–M).



In contrast, when subjected to a light pulse, flies explore the square blocks surrounding the activation zone, covering large search distances and frequently revisiting the activation zone (Figures 3I–M). These experiments demonstrate that flies can execute a local search without being able to freely choose the location, timing, or angle of their turns — further evidence that this behavior relies on path integration rather than a search algorithm that does not require spatial memory [5]. In open-arena experiments, flies generate highly tortuous searches, even while they are returning to the activation zone (e.g. Figure S1C), resulting in complex trajectories that are challenging to analyze. By constraining local search behavior into discrete runs and turns, the Flyadelphia assay opens the door to more interpretable manipulations via genetic tools as well as simplified agent-based models of path integration.

The ability to execute a sustained search centered around a fictive-food site in complete darkness, and moreover to carry this out in an environment with arbitrary geometric constraints, strongly suggests that flies can keep track of their location relative to the activation zone. This feat of idiothetic path integration has previously been compared to other insect behaviors such as the foraging excursions of desert ants (*Cataglyphis fortis*) [5], which routinely embark on long and winding runs through featureless terrain and yet are able to return to their nest in a direct path [50]. To accomplish this, these ants keep track of both the distance and the direction of their travel, enabling them to integrate their position relative to a point of origin [51–53]. During food-triggered searches, *Drosophila* may be using the same computational strategies as *Cataglyphis*, and thus may be relying on the same highly conserved brain structures [6, 7]. In particular, studies point to the importance of the central complex — a sensorimotor hub of the insect brain that processes numerous aspects of locomotion, navigation and decision-making [54]. Wedge neurons of the ellipsoid body encode azimuthal heading, potentially serving as a compass for path integration, celestial navigation, and other behaviors [55–58]. Whereas less is known about how insects monitor odometry, it is thought that step-counting can be achieved by using proprioceptive feedback or efferent copies of motor commands to integrate distance traveled [6, 52].

We propose that optogenetic activation of *Gr43a*- and *Gr5a-GAL4* sugar sensors may be a potent tool in future experiments seeking to characterize the neural implementation of path integration. Among the sensory pathways we studied, these sweet-sensing neurons are the most reliable triggers of local search. However, the comparatively weaker searches elicited by activation of other neural pathways in this study may be a consequence of differences in the levels or anatomical depth of transgene expression, rather than a reflection of their contribution to search behavior. Regardless of this experimental limitation, the fact that so many sensory modalities can trigger local searches suggests a convergence of these pathways onto the set of brain structures underlying navigation. This is consistent with anatomical studies of the central complex showing that it receives a variety of indirect sensory inputs [54], as well as direct innervation by a large subset of *NPF-GAL4* neurons [37, 59].

Elucidating the function of these circuits in path integration would require the ability to record neural activity in the *Drosophila* brain during local search. To this end, we developed a preparation to elicit local searches in a tethered fly walking on an air-suspended spherical treadmill (Figure 4A). Similar setups have been successfully used to examine the path

integration behavior of *Cataglyphis* ants [60]. The fly's fictive path was reconstructed in real-time using the FicTrac machine vision system [61], and a closed-loop program controlled optogenetic stimulation to present fictive food sites in the virtual 2-D environment. As the fly walked, it would at certain points receive optogenetic stimulation; this virtual location became a fictive food site with an activation zone, thus mimicking our free-walking experiments. If the fly strayed far away from the activation zone, the fictive food site was abolished and a new fictive food site was spawned soon after at the fly's new position. In this manner, flies experienced numerous virtual fictive food sites, and we later examined whether they performed local searches in each case. Trials included an initial baseline period and a final post-experimental period during which mock fictive food sites were created, but the fly received no activation.

Activation of *Gr43a-GAL4* sugar-sensors triggered local searches in the virtual environment that resembled searches in free-walking flies (Figure 4B, Video S4). The spatial scale of the searches was smaller than that of free-walking flies, perhaps due to increased error-accumulation in idiothetic path integration caused by a mismatch between the fly's intended locomotion and the machine-reconstructed fictive path. Nevertheless, compared to the baseline and post conditions, and unlike parental controls, these searches covered greater distances, consisted of numerous revisits to the activation zone and were highly centered at the fictive food site (Figures 4C–E), suggesting that flies walking on the treadmill apparatus are capable of performing idiothetic path integration. As in free-walking flies, activation of *Gr43a-GAL4* neurons in tethered flies elicited a reduction in walking speed (Figure 4F) and proboscis extension (data not shown), accompanied by a strong startle response. These results are consistent with a recent report, using a similar setup in which flies explore a virtual environment with visual features [62]. That study found that activation of sugar-receptors triggers local search in a virtual landscape and that visual landmarks do not contribute to this behavior, supporting the hypothesis that flies are performing idiothetic path integration. Adapting these setups for use with a 2-photon microscope may permit future studies to examine how sensory stimuli, reward signals, spatial information, and memory are encoded and integrated to produce path integration.

In summary, we found that hungry flies initiate a sustained local search when they experience a fictive food stimulus. This search behavior appears to constitute a generalized foraging response, as it can be triggered by multiple types of food-associated neurons including water-, sugar-, and vinegar-odor-sensing neurons, as well as hunger-signaling neurons of the central nervous system. Like local searches triggered by real food, optogenetically induced local searches are modulated by internal nutritional state and show key features of idiothetic path integration. Our results suggest that flies are able to keep track of their spatial position relative to a fictive food stimulus, even within a constrained maze. We demonstrate that long-lasting local search bouts can be initiated repeatedly by the brief activation of specific sets of neurons, and we developed a system to reconstitute this behavior in a tethered fly, thus establishing a promising entry point to tracing the neural pathways underlying path integration in insects.



## STAR METHODS

### CONTACT FOR REAGENT AND RESOURCE SHARING

Further information and requests for resources and reagents should be directed to and will be fulfilled by the Lead Contact, Michael H. Dickinson (flyman@caltech.edu).

### EXPERIMENTAL MODEL AND SUBJECT DETAILS

Unless otherwise noted, we conducted all experiments using 5-to-7-day-old female *Drosophila melanogaster* reared in darkness at 25°C. Experimental flies were reared on standard cornmeal fly food containing 0.2 mM all transretinal (ATR) (Sigma-Aldrich) and transferred 0–2 days after eclosion onto standard cornmeal fly food with 0.4 mM ATR. Standard food was supplemented with additional yeast. Experimental flies were obtained by crossing *20XUAS-CsChrimson-mVenus* (inserted into attP40) virgin females to males of each GAL4 driver line. Parental control flies were obtained by crossing *20XUAS-CsChrimson-mVenus* (inserted into attP40) virgin females to wild-type males, and by crossing males of each GAL4 driver line to wild-type virgin females. The wild-type strain (Canton-S) originated from the lab of Martin Heisenberg. To facilitate sorting and transferring of experimental flies, we briefly anesthetized them at 4°C on a cold plate.

Unless otherwise noted, we starved flies prior to experiments by housing them for 33–42 hours in a vial supplied with a tissue (KimTech, Kimberly-Clark) containing 1 ml of distilled water with 800 μM ATR. 7-day-starved flies were housed for 5 days in a vial supplied with a tissue containing 1 mL of 10% sucrose with 800 μM ATR, and then transferred for 33–42 hours to a vial supplied with a tissue containing 1 ml of distilled water with 800 μM ATR. In all cases, the conditioned tissue was replenished daily. Dry-starved flies were housed for 16–26 hours in a vial containing a desiccant (Drierite, W. A. Hammond) beneath a cotton ball. To specifically deprive flies of either sugar or protein, we prepared a synthetic food medium based on an existing protocol [44]. Agar concentration was increased 5-fold to achieve a suitable texture for the food, and 0.4 mM ATR was added to the prepared food. To deprive flies of sugar, we starved flies for 33–42 hours on synthetic media lacking sucrose. To deprive flies of protein, we starved flies for 7–8 days on synthetic media lacking casein — for these experiments, we tested 7–8-day-old flies. Compared to standard food, there was no apparent increase in mortality for flies housed on synthetic media lacking sugar or protein (data not shown). Green food dye (McCormick & Company) was added (2.5 ml/L) to the medium to visually confirm that flies were consuming the synthetic food (data not shown).

### METHOD DETAILS

**Behavioral experiments with free-walking flies**—Experiments were conducted in a circular chamber constructed from layers of acrylic (118 mm diameter, 2.75 mm high). We constructed the Flyadelphia chamber from layers of acrylic with insertable acrylic blocks to form the grid, such that flies were confined to the passages between blocks (1.85 mm wide, 2.75 mm high) but had sufficient space to walk forwards or backwards or turn around at any point in the arena. An upward-directed, custom-made array of 850 nm LEDs, covered by a translucent acrylic panel, was situated 11 cm beneath the arena to provide backlighting for a top-mounted camera (Blackfly, FLIR) recording at 30 frames per second. For optogenetic

stimulation, we positioned upward-directed 628 nm LEDs (CP41B-RHS, Cree, Inc.) at the center of each activation zone, 8.5 mm beneath the arena floor. We covered the chamber lid with a 3 mm thick long pass acrylic filter (color 3143, ePlastics). The chamber floor was transparent to allow for optogenetic stimulation, and a filter (#3000 Tough Rolux, Rosco Cinegel) was situated beneath the chamber to diffuse the red light used for stimulation. The camera, fly chamber, optogenetic stimulation lighting panel, and background lighting panel were held within a rigid aluminum frame (80/20), and the entire structure was covered with dense cloth to block any external light.

For each experiment, we aspirated a single fly into the behavioral chamber. Experiments began with an initial 10-minute baseline period, followed by 30 minutes during which the activation zone was operational. Experiments were terminated at the conclusion of this timeframe. Experiments in the Flyadelphia arena consisted either of 60-minute trials during which the activation zone was operational, or equivalent baseline control trials with no activation zone. Behavioral chambers were cleaned with 100% ethanol at the conclusion of each trial and allowed to dry before reuse. We tracked the 2-D position of the fly in real-time using a python-based machine vision platform built on the Robot Operating System ([http://florisvb.github.io/multi\\_tracker](http://florisvb.github.io/multi_tracker)) [64]. The tracking system was customized to implement closed-loop control of optogenetic stimulation via an LED controller (1031, Phidgets Inc). The LED beneath each activation zone was turned on for 1 second whenever the centroid of the fly entered its virtual perimeter (diameter 5.67 mm), except during the baseline period. Each 1-second pulse was followed by a 9-second refractory period during which the LED remained off, regardless of the fly's position. In preliminary experiments, in which we suspended optogenetic feedback after a single stimulation or after a few stimulations, the flies typically ceased searching soon thereafter (data not shown), perhaps because they did not receive the expected food stimulus upon their next return to the activation zone.

**Behavioral experiments with tethered flies**—For experiments using tethered flies, we starved flies 22–31 hours in a vial supplied with a tissue containing 1 ml of distilled water with 800  $\mu$ M ATR. If starvation lasted beyond 24 hours, the conditioned tissue was at that time replenished. We briefly anesthetized 3- to 7-day-old flies at 4°C on a cold plate and glued them to a tungsten wire at their dorsal surface anterior to the wings using UV-cured glue (Bondic, Inc.). We clipped the fly's wings to minimize attempted flight during experiments. We allowed the flies at least 30 minutes to recover and then allowed them 1–2 hours to acclimate after being placed on the spherical treadmill. Flies were excluded if they were frequently attempting to fly during the acclimation period. If a fly died during experiment, the trial was excluded. The tether was held by a micromanipulator, and we adjusted the fly's position on the ball using a side-view camera (Point Grey Blackfly, FLIR). The experiments were conducted inside a 30°C incubator (SRI6PF, Shellab), in complete darkness aside from the optogenetic stimulations. The ball for the spherical treadmill (5 mm radius) was fabricated from polyurethane foam (FR-7106, General Plastics), primed with white acrylic paint (Titanium White, Sargent Art Inc.) and then covered with an assortment of marks drawn with black acrylic paint (Ivory Black, Liquitex). The ball was air-suspended with 300 sccm flow in a custom-made housing attached to a mass flow controller (Allicat

Scientific). Fly virtual trajectories were reconstructed in real-time using the FicTrac machine vision software [61], via an overhead camera (Point Grey Blackfly, FLIR).

A closed-loop program ([https://github.com/willdickson/fictrac\\_vendomatic](https://github.com/willdickson/fictrac_vendomatic)) was used to present flies with fictive food sites in the 2-D virtual environment using a 625 nm light source aimed at the fly. A fictive food site consisted of a 5.67 mm diameter virtual activation zone. Whenever a fly entered the activation zone, it received a 1-second pulse of optogenetic stimulation, followed by a 9-second refractory period during which the stimulation remained off, regardless of the fly's virtual position. As the fly walked through the virtual environment, the system occasionally spawned a fictive food site at the fly's current position and then abolished it if the fly walked away. Specifically, the closed-loop system operated as follows. If no fictive food site was in existence for 10 seconds, the system spawned a fictive food site at the fly's current position, as long as the fly had walked 5 mm since the start of the 10 second period, and as long as the fly was currently moving. Each new fictive food site was abolished if the fly walked more than 60 mm away from it, and a new fictive food site was spawned in the manner described above. Thus, no more than one fictive food site existed in the virtual environment at any given time. Experiments began with an initial 10-minute baseline period, during which the fly received no optogenetic stimulation. This was followed by 30 minutes during which the optogenetic closed-loop system was operational. Trials ended with a 10-minute post-experimental control period equivalent to the baseline period. Any existing fictive food site was abolished at the conclusion of the baseline or activation periods, and a new fictive food site was spawned as described above.

**Proboscis extension experiments**—For proboscis extension reflex (PER) experiments, we briefly anesthetized flies at 4°C on a cold plate and glued them to a tungsten wire at their dorsal surface anterior to the wings using UV-cured glue (Bondic, Inc.). We allowed tethered flies at least 30 minutes to recover, and then positioned flies with their head 1.3 mm from a fiber optic 617 nm light source for optogenetic stimulation. Flies were subjected to five 1-second light pulses, each separated by 20 seconds. Experiments were recorded via an overhead camera (Blackfly, FLIR, 30 frames per second). To determine the percentage of stimuli eliciting PER for each fly, we manually scored whether each light pulse elicited a proboscis extension during the 5 seconds following light pulse onset.

## QUANTIFICATION AND STATISTICAL ANALYSIS

**Behavioral analysis of free-walking flies**—The dataset for each trial consisted of an array of X and Y coordinates representing the 2-D positions of the fly, as well as an array of LED states (on or off) for the activation zone(s). To process data, we discarded occasional frames where the fly was either not tracked, where a second object was tracked in addition to the fly (e.g. fly poop), or where the tracked position jumped more than 1.5 mm within two consecutive frames (e.g. due to sporadic tracking of another object). Because the sampling rate of tracking data was not precisely 30 Hz, we down-sampled and linearly interpolated all data to 20 Hz to generate a regularly sampled time series. We discarded any trials where the fly never encountered the activation zone during the activation period.

We classified the fly as being within one of three possible locations in the arena: at the arena edge, in the open-field portion of the arena, or in the activation zone. The fly was considered to be at the arena edge if it was within 5.27 mm from the wall of the arena. For experiments in the Flyadelphia arena, the arena edge was defined as all points more than 32.6 mm from the arena center. Otherwise, if the fly was not within the virtual perimeter of an activation zone, it was considered to be in the open-field portion of the arena. We used a Schmitt-trigger algorithm [65] to classify whether the fly was stopped or walking; a fly was considered to be stopped if its instantaneous speed fell below  $1 \text{ mm s}^{-1}$ , or walking if its instantaneous speed rose above  $3 \text{ mm s}^{-1}$ , and its classification state persisted when its speed fell between these thresholds.

We classified search bouts as any trajectories beginning with a light pulse and ending when the fly reached the arena edge or at the conclusion of the trial (Figure S1A). Equivalent bouts during baseline condition served as controls, and were defined as any trajectories beginning in the activation zone and ending when the fly reached the arena edge or at the conclusion of the trial. We divided search bouts into individual excursions from the activation zone, with each excursion counting as a revisit to the activation zone (Figures S1B and S1C). To implement this, we defined two radial distances from the activation zone to serve as thresholds, again using the logic of a Schmitt trigger. Excursions began when a fly that had entered the activation zone crossed the excursion threshold ring in the outbound direction, and ended when the fly crossed the excursion threshold ring in the inbound direction (inner radius, 5.67 mm; outer radius, 7.09 mm). Throughout the paper, all analyses in free-walking flies (unless otherwise noted) excluded search bouts truncated by the conclusion of the trial, as well as any timepoints when the fly was stopped or in the activation zone.

**Behavioral analysis of tethered flies**—Analysis of virtual local searches in tethered flies was similar to analysis of searches in free-walking flies. The dataset for each trial consisted of an array of X and Y coordinates representing the 2-D virtual positions of the fly, as well as an array of optogenetic stimulus states (on or off) and the virtual locations of the activation zones. We analyzed all search bouts, which we classified as trajectories beginning at the time a new fictive food site was spawned, and ending when the fly walked  $>30 \text{ mm}$  away from the fictive food site (virtual arena edge), or at the conclusion of the trial. We smoothed trajectories using a Kalman filter, and down-sampled and linearly interpolated all data to 40 Hz to generate regularly sampled time series. Activation zone revisits were determined as in free-walking flies, using an excursion threshold ring (inner radius, 3.5 mm; outer radius, 4.92 mm).

**Data reporting and statistical analysis**—We generated all figures using the python library FigureFirst [66]. Throughout the paper, 95% confidence intervals were calculated from distributions of median values generated by 1000 bootstrap iterations. Data replotted across figures may depict slightly differing 95% confidence intervals due to randomness inherent to the bootstrapping technique. Trials without a baseline control bout (i.e. the animal did not encounter the activation zone during the baseline period) or without a post-experimental control bout (in the case of tethered fly experiments) were excluded from pair-

wise Wilcoxon signed-rank tests. Throughout the paper, sample sizes refer to number of flies.

## DATA AND SOFTWARE AVAILABILITY

The data from this manuscript are published on Mendeley Data at doi:  
[10.17632/85wyz34nm6.1](https://doi.org/10.17632/85wyz34nm6.1)

## Supplementary Material

Refer to Web version on PubMed Central for supplementary material.

## ACKNOWLEDGEMENTS

We wish to thank Francesca V. Ponce for helpful discussions and assistance with preparing the synthetic food medium. Rubi Salgado assisted with fly rearing. Annie Rak helped with conducting the PER experiments. Ysabel M. Giraldo and Katherine J. Leitch provided advice on statistical analysis. Floris van Breugel and Theodore H. Lindsay helped implement the software used for tracking and closed-loop optogenetic stimulation. William B. Dickson created the software for closed-loop virtual fictive food sites, fabricated the balls for the spherical treadmill, and assisted in data analysis. Kristin Scott and John Carlson kindly provided us with flies. Research reported in this publication was supported by the National Institute of Neurological Disorders and Stroke of the National Institutes of Health under Award U19NS104655.

## REFERENCES

1. Pyke GH (1984). Optimal foraging theory: a critical review. *Ann Rev Ecol Syst* 15, 523–575.
2. Hassell MP, and Southwood TRE (1978). Foraging strategies of insects. *Ann Rev Ecol Syst* 9, 75–78.
3. Dethier VG (1957). Communication by insects: physiology of dancing. *Science* 125, 331–336. [PubMed: 17794437]
4. Dethier VG (1976). *The Hungry Fly* (Cambridge, MA: Harvard University Press).
5. Kim IS, and Dickinson MH (2017). Idiothetic path integration in the fruit fly *Drosophila melanogaster*. *Curr Biol* 27, 2227–2238.e3. [PubMed: 28736164]
6. Heinze S, Narendra A, and Cheung A (2018). Principles of insect path integration. *Curr Biol* 28, R1043–R1058. [PubMed: 30205054]
7. Dickinson MH (2014). Death Valley, *Drosophila*, and the Devonian toolkit. *Annu Rev Entomol* 59, 51–72. [PubMed: 24160432]
8. White J, and Tobin TR (1984). Local search in the housefly *Musca domestica* after feeding on sucrose. *J Insect Physiol* 30, 477–487.
9. Bell WJ, Cathy T, Roggero RJ, Kipp LR, and Tobin TR (1985). Sucrose-stimulated searching behaviour of *Drosophila melanogaster* in a uniform habitat: modulation by period of deprivation. *Anim Behav* 33, 436–448.
10. Murata S, Brockmann A, and Tanimura T (2017). Pharyngeal stimulation with sugar triggers local searching behavior in *Drosophila*. *J Exp Biol* 220, 3231–3237. [PubMed: 28684466]
11. Miyamoto T, Slone J, Song X, and Amrein H (2012). A fructose receptor functions as a nutrient sensor in the *Drosophila* brain. *Cell* 151, 1113–1125. [PubMed: 23178127]
12. Miyamoto T, and Amrein H (2014). Diverse roles for the *Drosophila* fructose sensor Gr43a. *Fly* 8, 19–25. [PubMed: 24406333]
13. Marella S, Fischler W, Kong P, Asgarian S, Rueckert E, and Scott K (2006). Imaging taste responses in the fly brain reveals a functional map of taste category and behavior. *Neuron* 49, 285–295. [PubMed: 16423701]
14. Dahanukar A, Lei Y-T, Kwon JY, and Carlson JR (2007). Two Gr genes underlie sugar reception in *Drosophila*. *Neuron* 56, 503–516. [PubMed: 17988633]

15. Nelson MC (1977). The blowfly's dance: role in the regulation of food intake. *J Insect Physiol* 23, 603–611.
16. Vargas MA, Luo N, Yamaguchi A, and Kapahi P (2010). A role for S6 kinase and serotonin in postmating dietary switch and balance of nutrients in *D. melanogaster*. *Curr Biol* 20, 1006–1011. [PubMed: 20471266]
17. Ribeiro C, and Dickson BJ (2010). Sex peptide receptor and neuronal TOR/S6K signaling modulate nutrient balancing in *Drosophila*. *Curr Biol* 20, 1000–1005. [PubMed: 20471268]
18. Toshima N, and Tanimura T (2012). Taste preference for amino acids is dependent on internal nutritional state in *Drosophila melanogaster*. *J Exp Biol* 215, 2827–2832. [PubMed: 22837455]
19. Steck K, Walker SJ, Itskov PM, Baltazar C, Moreira J-M, and Ribeiro C (2018). Internal amino acid state modulates yeast taste neurons to support protein homeostasis in *Drosophila*. *eLife* 7, 119.
20. Croset V, Schleyer M, Arguello JR, Gerber B, and Benton R (2016). A molecular and neuronal basis for amino acid sensing in the *Drosophila* larva. *Sci Rep* 6, 34871. [PubMed: 27982028]
21. Ganguly A, Pang L, Duong V-K, Lee A, Schoniger H, Varady E, and Dahanukar A (2017). A molecular and cellular context-dependent role for Ir76b in detection of amino acid taste. *Cell Rep* 18, 737–750. [PubMed: 28099851]
22. Sánchez-Alcañiz JA, Silbering AF, Croset V, Zappia G, Sivasubramaniam AK, Abuin L, Sahai SY, Münch D, Steck K, Auer TO, et al. (2018). An expression atlas of variant ionotropic glutamate receptors identifies a molecular basis of carbonation sensing. *Nat Commun* 9, 4252. [PubMed: 30315166]
23. Zhang YV, Ni J, and Montell C (2013). The molecular basis for attractive salt-taste coding in *Drosophila*. *Science* 340, 1334–1338. [PubMed: 23766326]
24. Hussain A, Zhang M, Üçpınar HK, Svensson T, Quillery E, Gompel N, Ignell R, and Grunwald Kadow IC (2016). Ionotropic chemosensory receptors mediate the taste and smell of polyamines. *PLoS Biology* 14, e1002454–30. [PubMed: 27145030]
25. Ahn J-E, Chen Y, and Amrein H (2017). Molecular basis of fatty acid taste in *Drosophila*. *eLife* 6, 44.
26. Kennedy JS, and Marsh D (1974). Pheromone-regulated anemotaxis in flying moths. *Science* 184, 999–1001. [PubMed: 4826172]
27. van Breugel F, and Dickinson MH (2014). Plume-tracking behavior of flying *Drosophila* emerges from a set of distinct sensory-motor reflexes. *Curr Biol* 24, 274–286. [PubMed: 24440395]
28. Jung S-H, Hueston C, and Bhandawat V (2015). Odor-identity dependent motor programs underlie behavioral responses to odors. *eLife* 4.
29. Álvarez-Salvado E, Licata AM, Connor EG, McHugh MK, King BM, Stavropoulos N, Victor JD, Crimaldi JP, and Nagel KI (2018). Elementary sensory-motor transformations underlying olfactory navigation in walking fruit-flies. *eLife* 7.
30. Semmelhack JL, and Wang JW (2009). Select *Drosophila* glomeruli mediate innate olfactory attraction and aversion. *Nature* 459, 218–223. [PubMed: 19396157]
31. Bell JS, and Wilson RI (2016). Behavior reveals selective summation and max pooling among olfactory processing channels. *Neuron* 91, 425–438. [PubMed: 27373835]
32. Badel L, Ohta K, Tsuchimoto Y, and Kazama H (2016). Decoding of context-dependent olfactory behavior in *Drosophila*. *Neuron* 91, 155–167. [PubMed: 27321924]
33. Hallem EA, and Carlson JR (2006). Coding of odors by a receptor repertoire. *Cell* 125, 143–160. [PubMed: 16615896]
34. Christiaens JF, Franco LM, Cools TL, De Meester L, Michiels J, Wenseleers T, Hassan BA, Yaksi E, and Verstrepen KJ (2014). The fungal aroma gene ATF1 promotes dispersal of yeast cells through insect vectors. *Cell Rep* 9, 425–432. [PubMed: 25310977]
35. Cameron P, Hiroi M, Ngai J, and Scott K (2010). The molecular basis for water taste in *Drosophila*. *Nature* 465, 91–95. [PubMed: 20364123]
36. Schoofs L, De Loof A, and Van Hiel MB (2017). Neuropeptides as regulators of behavior in insects. *Annu Rev Entomol* 62, 35–52. [PubMed: 27813667]



37. Shao L, Saver M, Chung P, Ren Q, Lee T, Kent CF, and Heberlein U (2017). Dissection of the *Drosophila* neuropeptide F circuit using a high-throughput two-choice assay. *Proc Natl Acad Sci USA* 114, E8091–E8099. [PubMed: 28874527]
38. Liu C, Plaçais P-Y, Yamagata N, Pfeiffer BD, Aso Y, Friedrich AB, Siwanowicz I, Rubin GM, Prémat T, and Tanimoto H (2012). A subset of dopamine neurons signals reward for odour memory in *Drosophila*. *Nature* 488, 512–516. [PubMed: 22810589]
39. Yamagata N, Ichinose T, Aso Y, Plaçais P-Y, Friedrich AB, Sima RJ, Prémat T, Rubin GM, and Tanimoto H (2015). Distinct dopamine neurons mediate reward signals for short- and long-term memories. *Proc Natl Acad Sci USA* 112, 578–583. [PubMed: 25548178]
40. Landayan D, Feldman DS, and Wolf FW (2018). Satiation state-dependent dopaminergic control of foraging in *Drosophila*. *Sci Rep* 8, 5777. [PubMed: 29636522]
41. Root CM, Ko KI, Jafari A, and Wang JW (2011). Presynaptic facilitation by neuropeptide signaling mediates odor-driven food search. *Cell* 145, 133–144. [PubMed: 21458672]
42. Beshel J, and Zhong Y (2013). Graded encoding of food odor value in the *Drosophila* brain. *J Neurosci* 33, 15693–15704. [PubMed: 24089477]
43. Corrales-Carvajal VM, Faisal AA, and Ribeiro C (2016). Internal states drive nutrient homeostasis by modulating exploration-exploitation trade-off. *eLife* 5, 119.
44. Reis T (2016). Effects of synthetic diets enriched in specific nutrients on *Drosophila* development, body fat, and lifespan. *PLoS One* 11, e0146758. [PubMed: 26741692]
45. Zhang W, Ge W, and Wang Z (2007). A toolbox for light control of *Drosophila* behaviors through Channelrhodopsin 2-mediated photoactivation of targeted neurons. *Eur J Neurosci* 26, 2405–2416. [PubMed: 17970730]
46. Inagaki HK, Ben-Tabou de-Leon S, Wong AM, Jagadish S, Ishimoto H, Barnea G, Kitamoto T, Axel R, and Anderson DJ (2012). Visualizing neuromodulation in vivo: TANGO-mapping of dopamine signaling reveals appetite control of sugar sensing. *Cell* 148, 583–595. [PubMed: 22304923]
47. Inagaki HK, Jung Y, Hoopfer ED, Wong AM, Mishra N, Lin JY, Tsien RY, and Anderson DJ (2013). Optogenetic control of *Drosophila* using a red-shifted channelrhodopsin reveals experience-dependent influences on courtship. *Nat Methods* 11, 325–332. [PubMed: 24363022]
48. Tao L, Ozarkar S, and Bhandawat V (2018). Statistical structure of locomotion and its modulation by odors. *bioRxiv.org*.
49. Saar M, Gilad T, Kilon-Kallner T, Rosenfeld A, Subach A, and Scharf I (2017). The interplay between maze complexity, colony size, learning and memory in ants while solving a maze: A test at the colony level. *PLoS One* 12, e0183753. [PubMed: 28837675]
50. Müller M, and Wehner R (1988). Path integration in desert ants, *Cataglyphis fortis*. *Proc Natl Acad Sci USA* 85, 5287–5290. [PubMed: 16593958]
51. Wehner R, and Müller M (2006). The significance of direct sunlight and polarized skylight in the ant's celestial system of navigation. *Proc Natl Acad Sci USA* 103, 12575–12579. [PubMed: 16888039]
52. Wittlinger M, Wehner R, and Wolf H (2006). The ant odometer: stepping on stilts and stumps. *Science* 312, 1965–1967. [PubMed: 16809544]
53. Wehner R, and Srinivasan MV (2003). Path integration in insects In “The Neurobiology of Spatial Behaviour.” pp. 9–30 Jeffery KJ, ed. (Oxford: Oxford University Press).
54. Pfeiffer K, and Homberg U (2014). Organization and functional roles of the central complex in the insect brain. *Annu Rev Entomol* 59, 165–184. [PubMed: 24160424]
55. Seelig JD, and Jayaraman V (2015). Neural dynamics for landmark orientation and angular path integration. *Nature* 521, 186–191. [PubMed: 25971509]
56. Green J, Adachi A, Shah KK, Hirokawa JD, Magani PS, and Maimon G (2017). A neural circuit architecture for angular integration in *Drosophila*. *Nature* 546, 101–106. [PubMed: 28538731]
57. Turner-Evans D, Wegener S, Rouault H, Franconville R, Wolff T, Seelig JD, Druckmann S, and Jayaraman V (2017). Angular velocity integration in a fly heading circuit. *eLife* 6, e04577.
58. Kim SS, Rouault H, Druckmann S, and Jayaraman V (2017). Ring attractor dynamics in the *Drosophila* central brain. *Science* 356, 849–853. [PubMed: 28473639]

59. Wen T, Parrish CA, Xu D, Wu Q, and Shen P (2005). *Drosophila* neuropeptide F and its receptor, NPFR1, define a signaling pathway that acutely modulates alcohol sensitivity. *Proc Natl Acad Sci USA* 102, 2141–2146. [PubMed: 15677721]
60. Dahmen H, Wahl VL, Pfeffer SE, Mallot HA, and Wittlinger M (2017). Naturalistic path integration of *Cataglyphis* desert ants on an air-cushioned lightweight spherical treadmill. *J Exp Biol* 220, 634–644. [PubMed: 28202651]
61. Moore RJD, Taylor GJ, Paulk AC, Pearson T, van Swinderen B, and Srinivasan MV (2014). FicTrac: a visual method for tracking spherical motion and generating fictive animal paths. *J Neurosci Methods* 225, 106–119. [PubMed: 24491637]
62. Haberkern H, Basnak MA, Ahanonu B, and Schauder D (2018). On the adaptive behavior of head-fixed flies navigating in two-dimensional, visual virtual reality. [biorxiv.org](https://doi.org/10.1101/282026).
63. Weiss LA, Dahanukar A, Kwon JY, Banerjee D, and Carlson JR (2011). The molecular and cellular basis of bitter taste in *Drosophila*. *Neuron* 69, 258–272. [PubMed: 21262465]
64. van Breugel F, Huda A, and Dickinson MH (2018). Distinct activity-gated pathways mediate attraction and aversion to CO<sub>2</sub> in *Drosophila*. *Nature* 564, 420–424. [PubMed: 30464346]
65. Robie AA, Straw AD, and Dickinson MH (2010). Object preference by walking fruit flies, *Drosophila melanogaster*, is mediated by vision and graviperception. *J Exp Biol* 213, 2494–2506. [PubMed: 20581279]
66. Lindsay T, Weir PT, and van Breugel F (2017). FigureFirst: A layout-first approach for scientific figures. *Proc. of the 15th Python in Science Conf* doi:10.25080/shinma-7f4c6e7-009

**HIGHLIGHTS**

- Local search bouts are triggered by brief activation of diverse sensory pathways
- Search trajectories exhibit hallmarks of idiothetic path integration
- Flies can perform local search in a confined maze or on a spherical treadmill
- Optogenetically induced local searches offer a tractable model of insect navigation

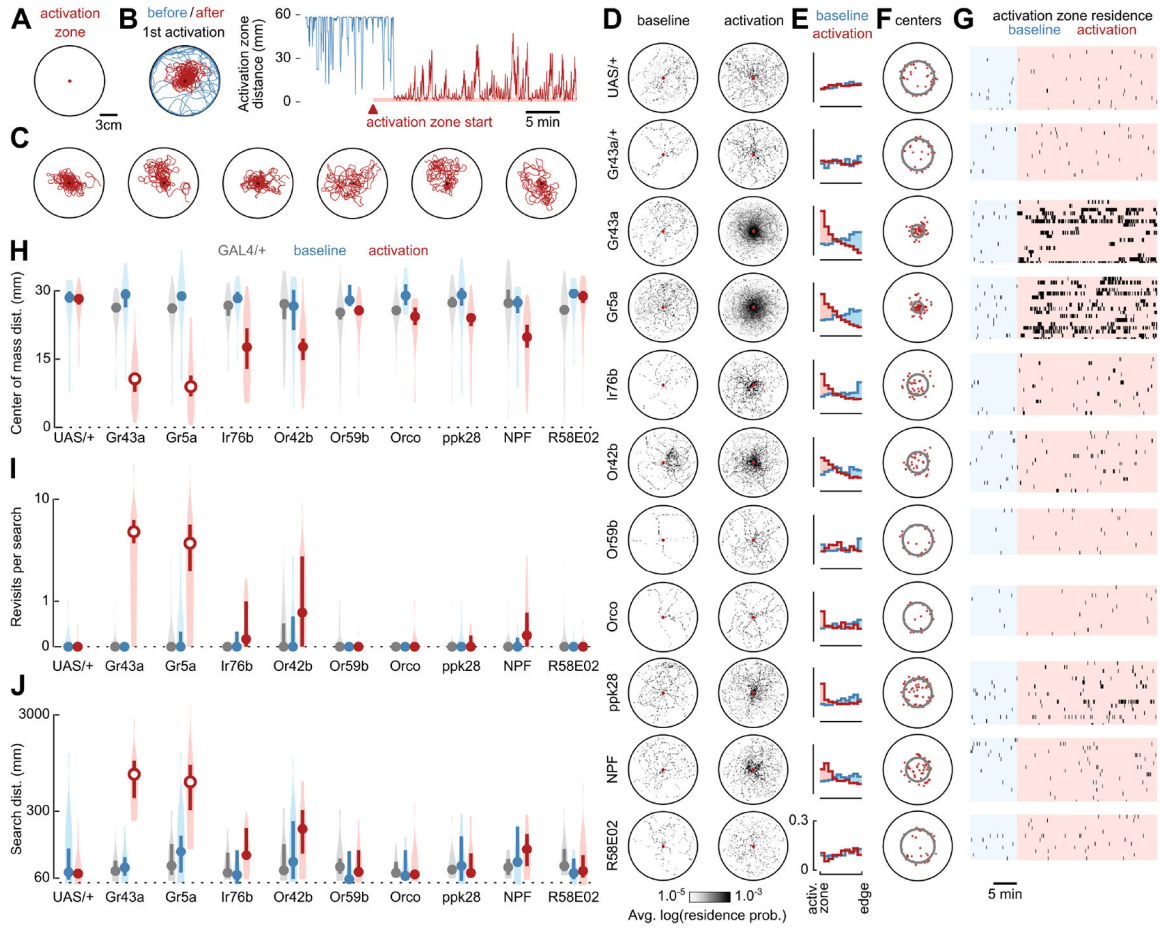


**Figure 1. Optogenetic activation of sugar-receptors triggers local search.**

(A) Schematic of experimental arena featuring an optogenetic activation zone. A female *Drosophila* is about 3 mm in length.

(B) Left: example trajectory of *Gr43a-GAL4>UAS-CsChrimson* fly before (blue) and after (red) first optogenetic stimulation. Right: the same data, plotted as the distance between the fly and activation zone center. The activation zone becomes operational after an initial 10-minute baseline control period.

(C) Six of the seven longest distance search bouts (left to right) triggered by *Gr43a-GAL4* activation; the longest bout is plotted in (B). Data include search bouts truncated by the conclusion of the trial.

(D) Residence probabilities of walking trajectories during activation search bouts (with light pulses) and baseline control bouts (without light pulses). Each 2-D spatial probability histogram shows the mean of the mean normalized residence probability distribution of each fly. Throughout the paper (unless otherwise noted), analyses in free-walking flies excluded search bouts truncated by the conclusion of the trial, as well as any timepoints when the fly was stopped or in the activation zone. UAS/+ indicates data for *UAS-CsChrimson*;+ parental controls. Gr43a/+ (for example) indicates data for *Gr43a-GAL4*;+ parental controls whereas Gr43a indicates corresponding data for *Gr43a-GAL4>UAS-CsChrimson* experimental flies.

(E) Probability distributions of distance between fly and activation zone during activation search bouts (red) or baseline control bouts (blue). Each probability histogram shows the mean of the mean normalized probability distribution of each fly.

(F) Centers of mass for all activation search bouts (red dots). Grey rings show the distance from the activation zone of the median center of mass.

(G) Raster plots of activation zone residence during baseline (blue) and while the activation zone is operational (red). Marks are graphically extended horizontally by 5 seconds for visibility.

(H) Distance from the arena center for centers of mass of baseline control bouts (blue), activation search bouts (red) and activation search bouts of GAL4-line parental controls (grey). Circles depict medians, error bars depict 95% confidence intervals, and violin plots indicate full data distribution. Unfilled circles indicate cases in which the median is statistically different ( $p < 0.05$ , with Bonferroni correction) from both baseline condition (Wilcoxon signed-rank test) and GAL4-line parental control (where applicable, Mann-Whitney U test).

(I) Mean number of revisits to the activation zone (plotted on a log axis) during baseline control bouts (blue), activation search bouts (red), and activation search bouts of GAL4-line parental controls (grey). Plotting conventions as in (H).

(J) Mean distance walked (plotted on a log axis) during baseline control bouts (blue), activation search bouts (red), and activation search bouts of GAL4-line parental controls (grey). Plotting conventions as in (H).

(C-J) Sample sizes (throughout paper, expressed as number of flies): Gr43a, n=20; Gr43a/+, n=15; UAS/+, n=23; Gr5a, n=20; Gr5a/+, n=16; Ir76b, n=16; Ir76b/+, n=12; Or42b, n=16; Or42b/+, n=13; Or59b, n=12; Or59b/+, n=18; Orco, n=13; Orco/+, n=18; ppk28, n=18; ppk28/+, n=14; NPF, n=18; NPF/+, n=11.

See also Figures S1 and S2.

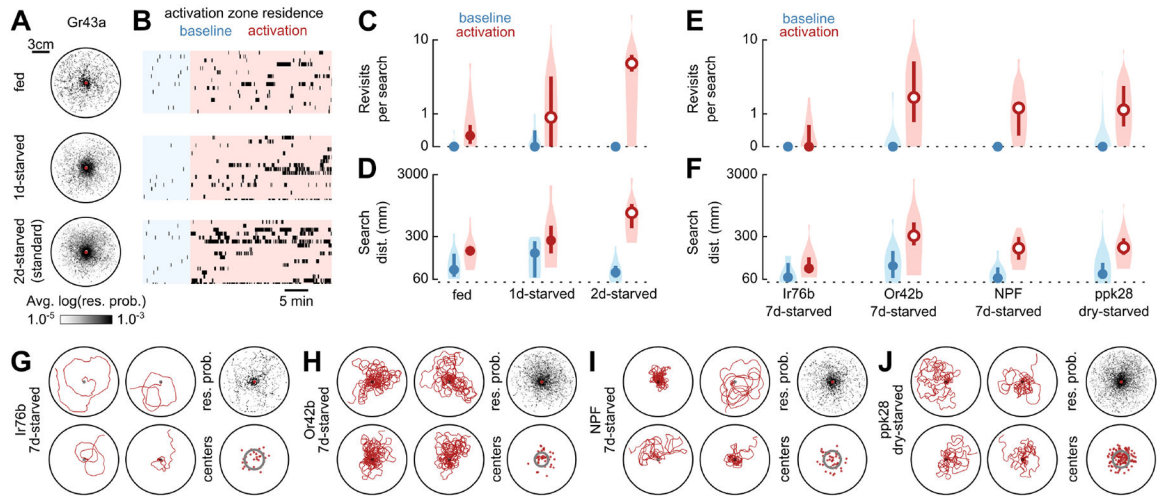


**Figure 2. Local searches are augmented by starvation and can be triggered by a variety of food-associated neurons.**

(A) Residence probabilities during activation search bouts for *Gr43a-GAL4>UAS-CsChrimson* animals reared continually on food (fed, n=16), starved for 9–18 hours (1d-starved, n=18), or starved for our standard 33–42 hours (2d-starved, n=20), plotted as in Figure 1D. 2d-starved data are replotted from Figures 1D–1J for convenience.

(B) Raster plots of activation zone residence for data in (A), plotted as in Figure 1G.

(C) Mean number of revisits to the activation zone for data in (A), plotted as in Figure 1I.

(D) Mean distance walked during search bouts for data in (A), plotted as in Figure 1J.

(E) Mean number of revisits to the activation zone for animals of the indicated genotype and starvation state, plotted as in Figure 1I.

(F) Mean distance walked during search bouts for animals of the indicated genotype and starvation state, plotted as in Figure 1J.

(G) Longest distance search bouts (left, clockwise from top-left, plotted as in Figure 1C), residence probabilities (top-right, plotted as in Figure 1D), and centers of mass (bottom-right, plotted as in Figure 1F), for activation search bouts of 7-day-starved *Ir76b-GAL4>UAS-CsChrimson* animals.

(H) As in (G) for 7-day-starved *Or42b-GAL4>UAS-CsChrimson* animals. (I) As in (G) for 7-day-starved *NPF-GAL4>UAS-CsChrimson* animals.

(J) As in (G) for dry-starved *ppk28-GAL4>UAS-CsChrimson* animals.

(E–J) Sample sizes: Ir76b 7d-starved, n=15; Or42b 7d-starved, n=13; NPF 7d-starved, n=11; ppk28 dry-starved, n=25.

See also Figures S3 and S4.



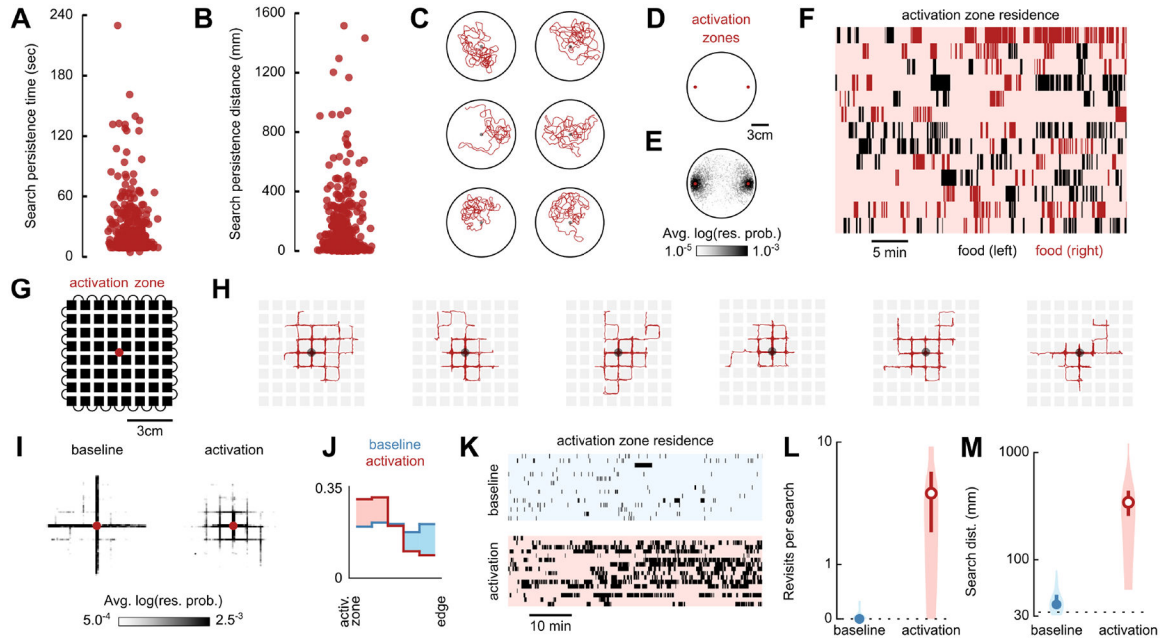


**Figure 3. Flies keep track of fictive-food location, even in a confined maze.**

(A) Persistence of search excursions without intervening optogenetic stimulation, shown as the durations of all trajectories beginning at the offset of a light pulse and ending with onset of the subsequent light pulse or conclusion of search bout, for *Gr43a-GAL4>UAS-CsChrimson* animals. Data are from experiments in Figure 1, and include residence in the activation zone and search bouts truncated by the conclusion of the trial.

(B) Distance walked for each trajectory plotted in (A).

(C) Longest distance trajectories (clockwise from top-left) from data in (B).

(D) Schematic of experimental arena with two optogenetic activation zones. (E) Residence probability with two activation zones as in (D), during activation search bouts for *Gr43a-GAL4>UAS-CsChrimson* animals (n=13). Plotted as in Figure 1D.

(F) Raster plots of residence in both activation zones for data in (E), plotted as in Figure 1G. (G) Schematic of Flyadelphia experimental arena featuring an optogenetic activation zone. Flies are restricted to the narrow passages between the blocks of the grid (black). *Gr43a-GAL4>UAS-CsChrimson* animals were used in all experiments, and trials consisted of either baseline (no optogenetic stimulation, n=15) or activation condition (n=16).

(H) Longest distance search bouts (from left to right, plotted as in Figure 1C).

(I) Residence probability during search bouts, plotted as in Figure 1D.

(J) Probability distributions of fly distance to the activation zone, plotted as in Figure 1E.

(K) Raster plots of activation zone residence during baseline (top) or activation (bottom) experiments, plotted as in Figure 1G.

(L) Mean number of revisits to the activation zone during search bouts. Plotted as in Figure 1I. Unfilled circles indicate that the median is statistically different ( $p < 0.05$ ) from baseline condition (Mann-Whitney U test).

(M) Mean distance walked during search bouts, plotted as in Figure 1J, statistics as in (L).

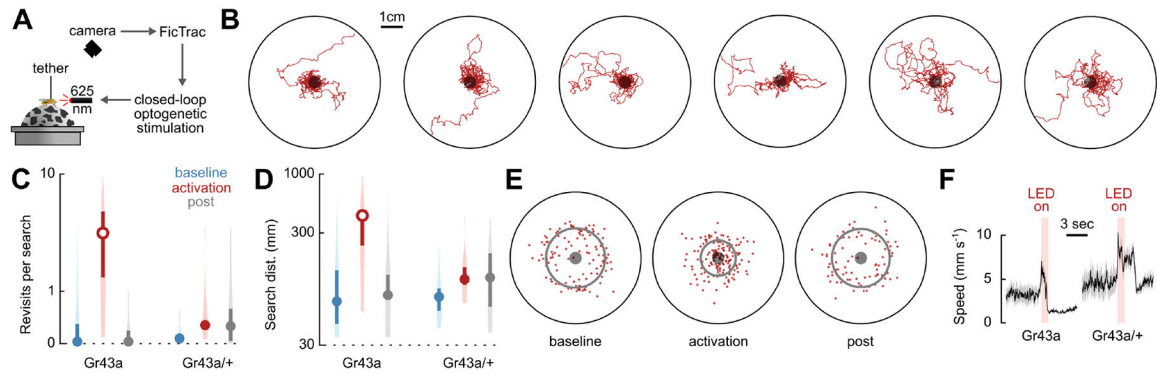


**Figure 4. Optogenetically induced virtual local search in a tethered fly.**

(A) Schematic of virtual reality system to study path integration in a tethered fly. The fly walks on an air-suspended spherical treadmill, and its fictive path is reconstructed in real-time using an overhead camera and FicTrac machine vision software [61]. A closed-loop program presents fictive food sites in the virtual 2-D environment by controlling optogenetic activation of *Gr43a-GAL4* sugar-sensing neurons.

(B) Longest distance search bouts (from left to right, plotted as in Figure 1C). Outer ring represents virtual arena edge.

(C) Mean number of revisits to the activation zone during search bouts for *Gr43a-GAL4>UAS-CsChrimson* animals (n=18) or *GAL4* parental control animals (n=13), plotted as in Figure 1I. Trials included two 10-minute control periods during which animals received no optogenetic stimulation: an initial baseline period (blue) and a final post-experimental period (grey). Unfilled circles indicate that the median is statistically different from both baseline and post-experimental condition (Wilcoxon signed-rank test, p 0.05, with Bonferroni correction).

(D) Mean distance walked during search bouts, plotted as in Figure 1J, statistics as in (C).

(E) Centers of mass for all activation search bouts, plotted as in Figure 1F. (F) Median speed traces during light pulse stimulation for animals of the indicated genotype, plotted as in Figure S4B.